NASA-CR-194572

/N-/ 43-/
190560
10 P

SEA ICE MOTIONS IN THE CENTRAL ARCTIC ICE CENTRAL ARCTIC PACK ICE AS INFERRED FROM AVHRR IMAGERY

Annual Progress Report

to the

National Aeronautics and Space Administration

Grant No. NAGW-2948

October 1993

William Emery, James Maslanik, Charles Fowler

Colorado Center for Astrodynamics Research
University of Colorado
Boulder, Colorado 8030

(NASA-CR-194572) SEA ICE MOTIONS IN THE CENTRAL ARCTIC ICE CENTRAL ARCTIC PACK ICE AS INFERRED FROM AVHRR IMAGERY Annual Progress Report (Colorado Univ.) 10 p

N94-15701

Unclas

G3/48 0190560

1.0 Rationale and Objectives

Synoptic observations of ice motion in the Arctic Basin are currently limited to those acquired by drifting buoys and, more recently, radar data from ERS-1. Buoys are not uniformly distributed throughout the Arctic, and SAR coverage is limited regionally and temporally due to the data volume, swath width, processing requirements, and power needs of the SAR. Additional ice-motion observations that can map ice responses simultaneously over large portions of the Arctic on daily to weekly time intervals are thus needed to augment the SAR and buoy data and to provide an intermediate-scale measure of ice drift suitable for climatological analyses and ice modeling.

Merging the remotely-sensed ice motions with SAR, AVHRR, OLS, and SSM/I imagery permits studies of ice processes over a range of space and time scales. A medium-resolution passive microwave sensor might be ideal for this purpose, but no such satellite will be available in the near future. Combinations of existing data types are thus likely to be our best bet for generating motion fields with a coverage and resolution best suited to climate studies.

Principal objectives of this project are to: 1) demonstrate whether sufficient ice features and ice motion existed within the consolidated ice pack to permit motion tracking using AVHRR imagery; 2) determine the limits imposed on AVHRR mapping by cloud cover; and 3) test the applicability of AVHRR-derived motions in studies of ice-atmosphere interactions.

2.0 Methodology

To meet these objectives, AVHRR data for portions of the Arctic Ocean have been acquired from several sources, including Greenland Sea coverage during CEAREX (60 days), daily coverage for the Beaufort Sea (one orbit per day for June 1992 - August 1993) purchased by special arrangement from the Canadian Atmospheric Environment Service (AES) at Edmonton, selected areas obtained from the EROS Data Center in Sioux Falls, South Dakota, and the AVHRR Arctic coverages for 1989 produced by the Naval Research Laboratory as part of the Leads program (Fetterer and Hawkins, 1991) . Other data used included 158 SAR motion vector files, SAR lo-res images, AOBP buoy tracks for 1991-1992, NMC gridded pressures and winds, ice-model output fields, and SSM/I data through 1991.

To determine ice velocities, two-dimensional cross correlations are used to match feature locations between pairs of co-registered images typically separated by one to three days (Emery et al., 1991a). This method has been used for many different purposes, such as image registration, cloud tracking, and determining velocity vectors from AVHRR and SAR data (Ninnis et al., 1986; Kwok, et al., 1990). Vectors are filtered based on the local cross-correlation coefficient and correlation of individual vectors with neighboring vectors. Ice motions have currently been calculated in this manner for several case studies such as the October 1991 period described below, and for a six-month period using the Beaufort Sea coverage.

2.1 Data Issues

We find cloud cover to be the only limiting factor for producing AVHRR-derived ice motions. Geolocation, feature identification, and sampling time otherwise appear adequate to yield detailed motion fields under all ice conditions studied. Cloud cover is regionally and seasonally dependent. For example, only 2 days out of the 60-day CEAREX data set for the Greenland Sea was sufficiently clear to yield useful ice motions. However, for the 97 days of available imagery in June - December 1992 for the Beaufort, motions were calculated for more than 50% of the region for 36 days, with areas of at least several thousand km^2 mapped for 80 of the 97 days. The effects of cloud cover are reduced by the ability of the correlation technique to track features visible through low-opacity cloud. Image processing steps can enhance the visibility of surface features, but these steps have not proven to be necessary. The Leads data set which consists of imagery spaced fairly far apart in time also yielded some useful motions elsewhere in the Arctic, but more frequent coverage is needed to minimize the effect of cloud cover.

In terms of data collection, processing, and archiving requirements, precise geolocation is required and as many orbits as possible should be collected. However, calibrated data are not necessary, GAC resolution yields useful ice motions, and the degradation of AVHRR field-of-view at off-angles from nadir appears to have no noticeable effect on the motion calculations. In terms of ice-motion products from AVHRR, data centers should therefore focus most effort on archiving multiple orbits and achieving high geolocation accuracy.

2.2 Comparisons of Remotely-Sensed, Observed, and Modeled Ice Motions

Figure 1 depicts how the scale of AVHRR fills a gap between the scales of SAR, buoy, and simulated ice motions. Shown are motions derived from AVHRR, from ERS-1 SAR generated by the ASF Geophysical Processing System (GPS), from AOBP buoy trajectories (Fig. 1a) and modeled ice motions (Fig. 1b) for a case study in October 1991. The AVHRR-derived ice motions fit nicely in terms of spatial scale and temporal coverage between the detailed resolution but less frequent time sampling of SAR, the high temporal resolution but widely-spaced buoy trajectories, and the daily, low-resolution velocity fields produced by the ice model. Comparisons of the AVHRR, SAR, buoy-derived ice motions, and simulations using different ice rheologies (e.g., viscous-plastic versus cavitating fluid) shows that all the motion products agree reasonably well in terms of drift direction and velocities. In particular, the AVHRR motions provide a valuable big-picture summary of drift conditions. This broader spatial coverage coincident in time permits a better overall comparison of the observed and modeled ice velocities than with the SAR or buoy data alone. For example, while the viscous-plastic and cavitating fluid rheologies yield nearly identical drift directions for the cases studied, the cavitating fluid rheology tends to overestimate drift speed during periods of strong ice motion.

This large-area view as well as the usefulness of the AVHRR-motions for identifying interesting local features are also demonstrated in Figure 2 for July 1992. For example, a mesoscale ice-motion pattern is apparent west of Banks Island, where the overall clockwise motion of the pack appears to be flowing around an "immobile" area (Fig. 2a; marked with an "X"). Twelve days later (Fig. 2b), this immobile region (or a similar one) is shifted to the southeast. Comparisons to other data are needed to tell whether this is a surface feature, an effect of local wind patterns, or some type of residual cloud effect.

2.3 *Creation of Uniform Gridded Fields of Ice Motion*

Work is underway to investigate the utility of combining ice motions from AVHRR, SAR, and drifting buoys into a uniform field suitable for ice-atmosphere studies and modeling. Even when cloud fraction is large, small patches of clear sky or thin cloud often allow motions to be calculated from AVHRR for small areas. When used alone, these patches do not provide the desired overall view of the ice pack, although they may be equivalent to isolated buoy or SAR observations. In some regions where cloud cover is very persistent (such as the Greenland Sea in the CEAREX data) other data types may be the only source of motions for the gridded product. One way of taking full advantage of all data sets and to cover as much of the Arctic as possible is to combine the AVHRR motions with other observations into an interpolated motion field. Our estimates of serial and spatial autocorrelations in buoy trajectories suggest that motions are correlated significantly over space scales of about 600 km and time periods of about 6 days. Ideally, sampling is needed at these intervals to generate a uniform motion grid. Optimal interpolation of buoy and SAR motions yields a gridded field (Fig. 3a) that is similar to an interpolated field from AVHRR alone (Fig. 3b) and comparable to the modeled ice motions in Fig. 1b. We therefore expect that combinations of the three observation types should yield useful gridded fields for modeling applications. Winds could be combined with the motion observations in areas where little confidence can be placed in the observations (e.g., at the grid cells indicated by large boxes in Fig. 3b). Alternatively, simulated ice motions that would presumably represent ice motion better than wind fields alone (particularly in non-free drift conditions) could be used as interpolation input.

3.0 **Summary of Work to Date**

The following are the major results of our current work:

a) Under clear-sky conditions or when cloud cover is sufficiently thin so that surface features are visible, accurate and detailed ice motions can be estimated from AVHRR HRPT, LAC and GAC data for the consolidated ice pack, based on comparisons to SAR and buoy-derived motions, and geostrophic winds;

b) Derivations of ice motions from AVHRR requires archiving of all available AVHRR orbits, although processing of these data, other than geolocation and the motion calculations themselves, is minimal;

c) AVHRR data alone can provide ice-motion coverage suitable for case studies of ice-atmosphere processes. However, combination with other data types is needed to provide daily, large-area coverage of ice motions;

d) The scale of AVHRR-derived motions is well-suited to regional studies and complements the higher-resolution SAR motions and low-resolution buoy coverage;

e) Optimally-interpolated motion fields that combine motions from AVHRR, SAR, and buoy observations can yield realistic, daily motion fields for large areas; and,

f) Limited comparison of the observed motions to simulations using a dynamic-thermodynamic ice model indicate good overall agreement in speed and direction. The use of a viscous-plastic versus cavitating fluid ice rheology has little effect on drift direction, but the cavitating fluid rheology appears to overestimate drift speed under conditions of rapid motion.

4.0 Planned Activities

During the next six months, the following tasks will be carried out:

- examination correlations over space and time to determine suitable sampling intervals for interpolations;

- complete motion calculations and generate interpolated fields from the June 1992 - Aug. 1993 data;
- estimate divergences from the interpolated fields;
- compare ice vectors with NMC and EMCWF winds and ice model output;
- generate a "film-loop" of a time series of ice motions to highlight variability of the ice pack;
- complete two publications describing the generation and application of the AVHRR-derived ice motions.

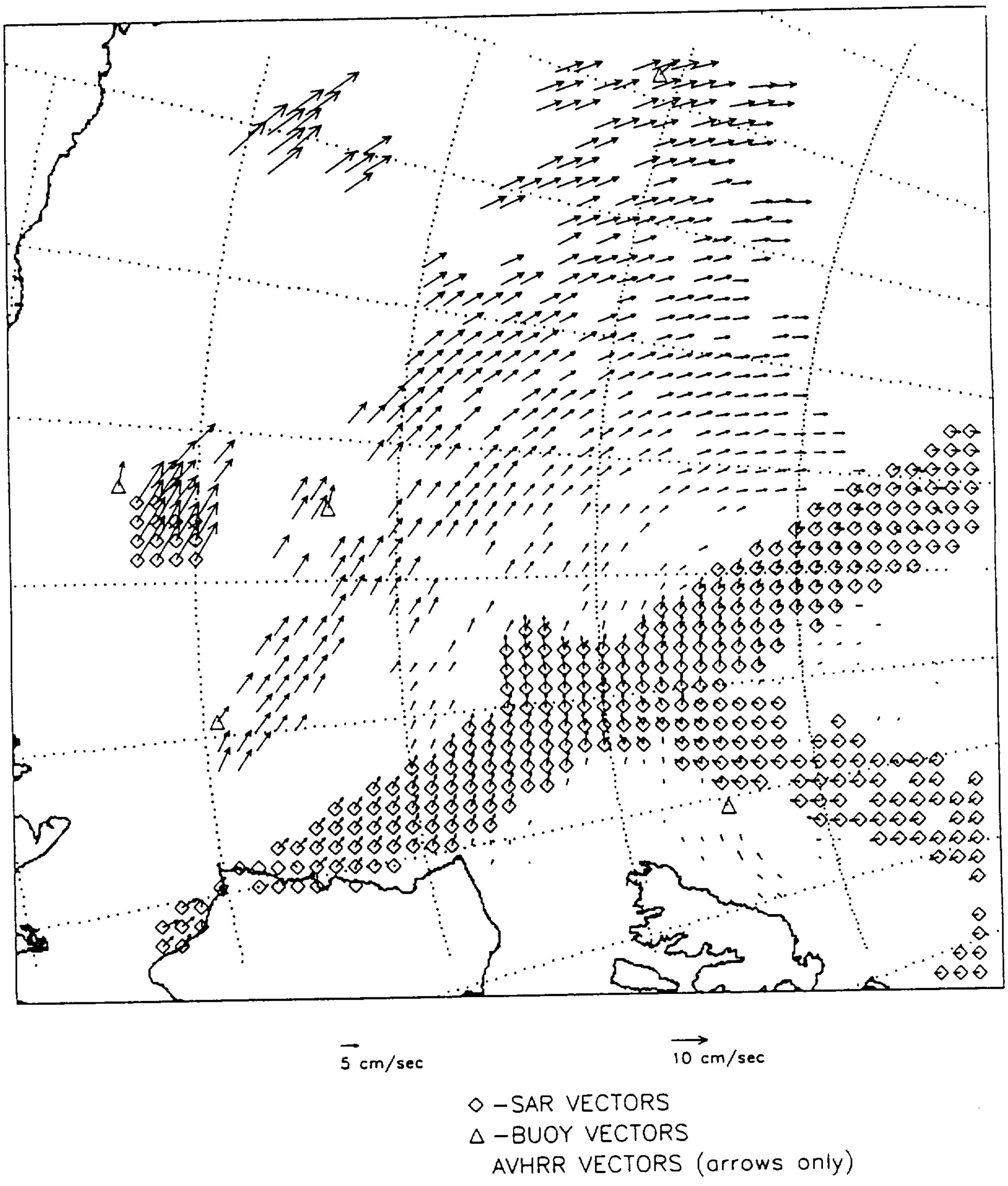

Figure 1a. Plots of ice-motion vectors derived from SAR, drifting buoys, and AVHRR for the Beaufort Sea. SAR vectors represent motion between Julian days 300 (27 Oct.) and 303, 1991 (every fifth vector is plotted). AVHRR and buoy data span days 298 to 302.

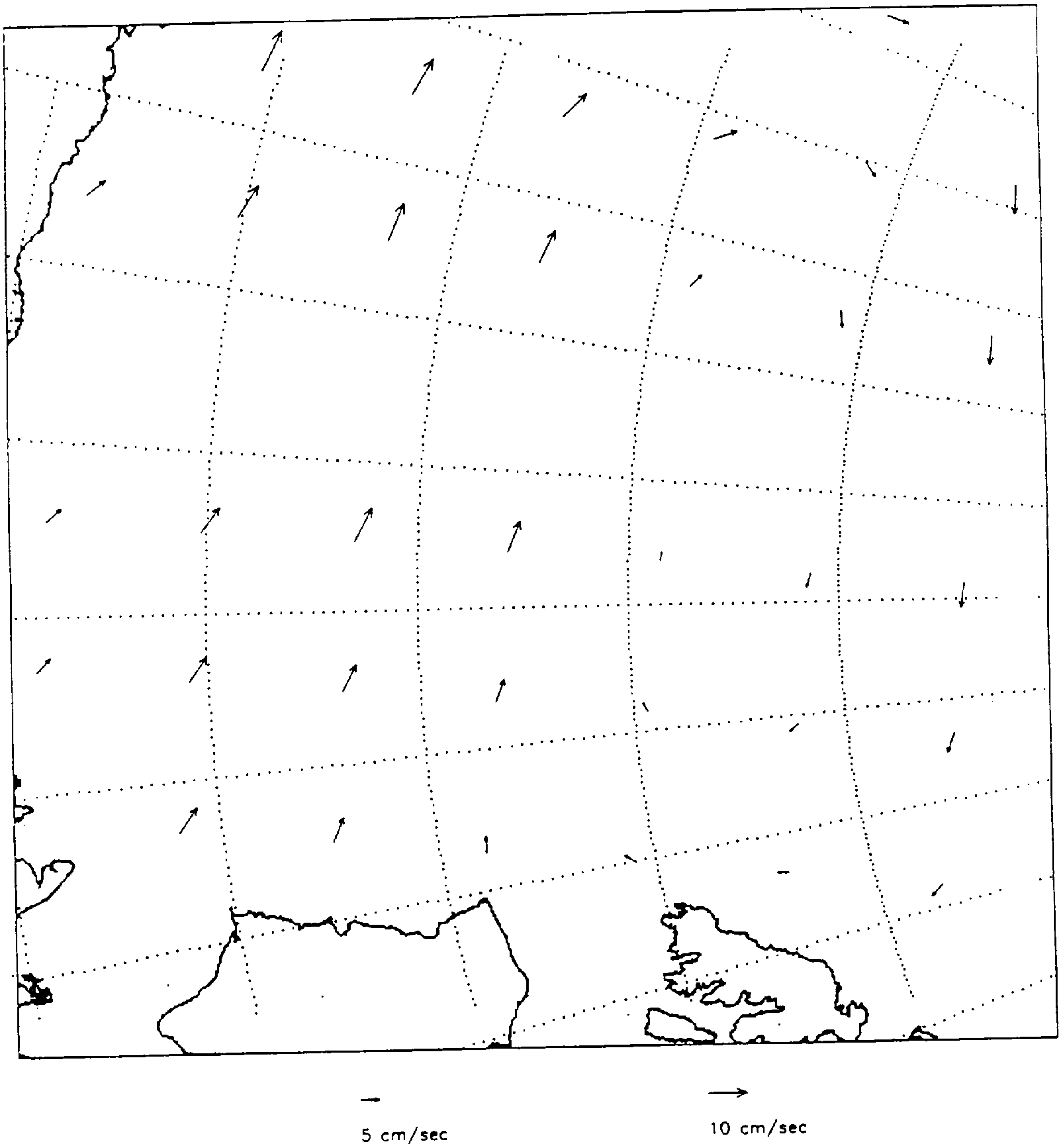

Figure 1b. Ice motions simulated using a viscous-plastic rheology and NMC winds for Julian days 298 to 302.

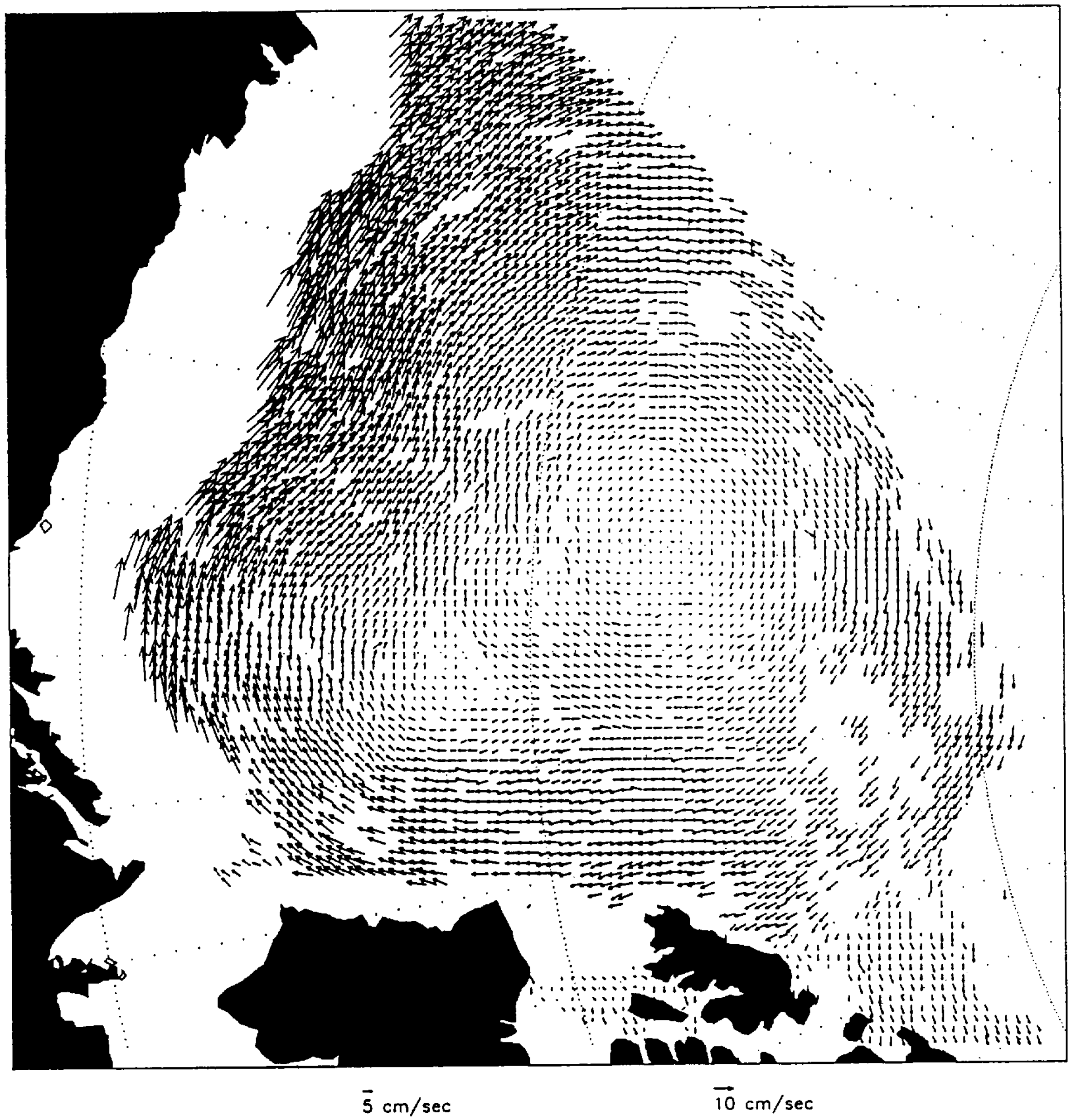

Figure 2a. Ice motions derived from sequential AVHRR images (e.g., motion over a one-day period) for Julian days 186-187 (5-6 July). A region of "immobile ice" is marked by an "X."

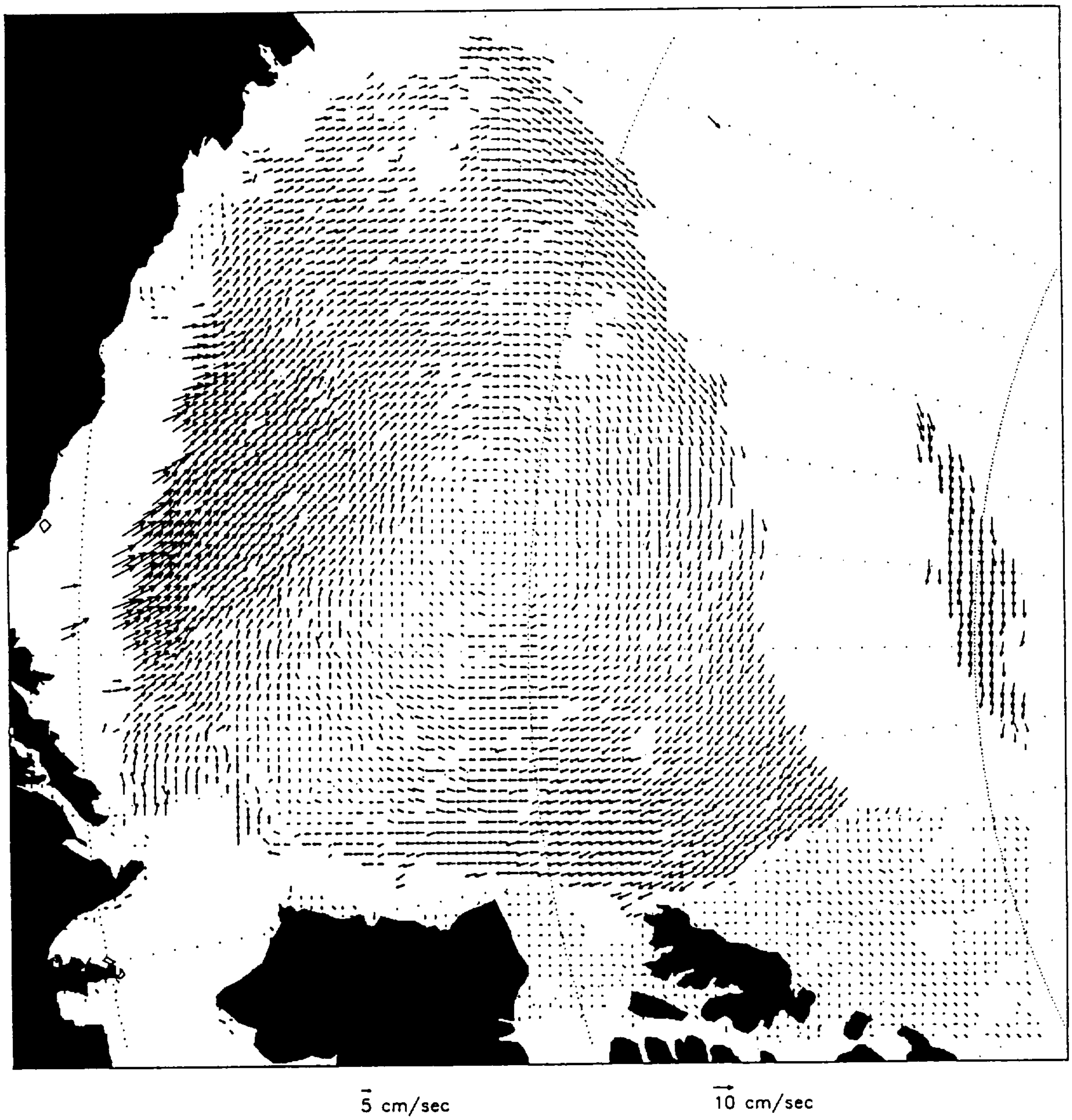

Figure 2b. AVHRR-derived ice motions as in Fig. 2a but for days 198-199 (17-18 July). A region of "immobile ice" is marked by an "X."

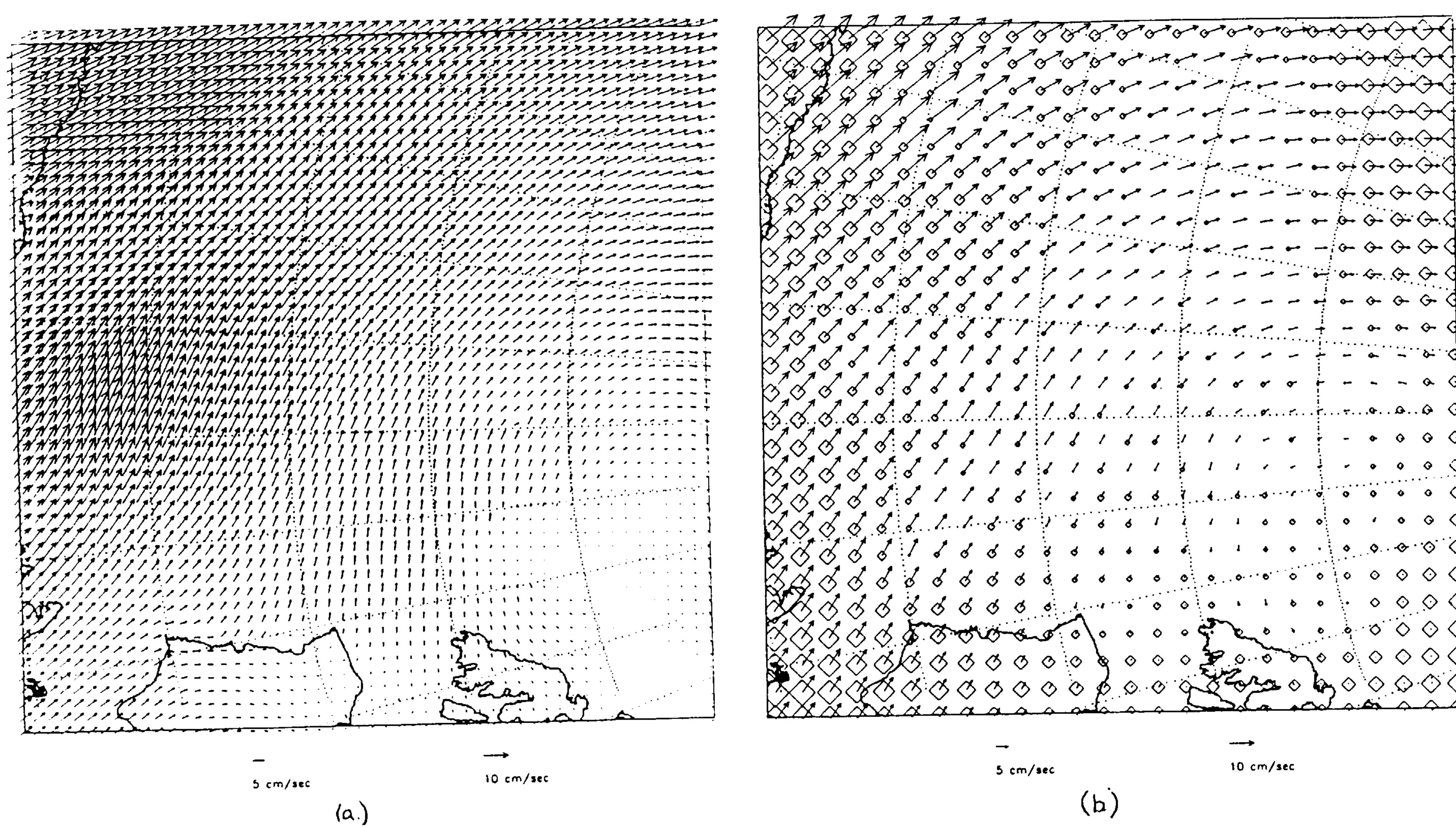

Figure 3. Ice motions on a uniform grid optimally interpolated from SAR and buoy data (Fig. 3a) and from AVHRR data only (Fig. 3b). Uncertainty in the interpolated vectors are indicated by the size of the diamond symbol at each grid point in Fig. 3b.